Supplementary Information
"The role of substrate mechanics in osmotic biofilm spreading"

Anthony Pietz,[a] Karin John,[*b] and Uwe Thiele[‡ac]

S1 Dimensionless model equations

Starting out from Eqs. (1)-(16) in section 2 of the main text we derive here the evolution equations for h, Ψ and ξ in their dimensionless form. In a first step we rewrite Eqs. (7)-(9) of the main text in a more convenient form

$$\partial_t h = -\nabla . \mathbf{j}_{\text{conv}} + j_o \tag{1}$$

$$\partial_t \Psi = -\nabla . (\phi \mathbf{j}_{\text{conv}} + \mathbf{j}_{\text{diff}}) + j_g \tag{2}$$

$$\partial_t \xi = j_s \,. \tag{3}$$

with the convective flux $\mathbf{j}_{\text{conv}}$

$$\mathbf{j}_{\text{conv}} = -\frac{h^3}{3\eta} \nabla \left[\partial_h f_w - \gamma_h \Delta (h + \xi) \right] , \tag{4}$$

the diffusive flux $\mathbf{j}_{\text{diff}}$

$$\mathbf{j}_{\text{diff}} = -D h \phi \nabla \partial_\phi f_m \,, \tag{5}$$

and the substrate motion

$$j_s = -\frac{1}{\zeta} \left[\kappa_v \xi - \gamma_h \Delta (h + \xi) - \gamma_\xi \Delta \xi \right] . \tag{6}$$

The osmotic flux j_o and the biomass growth j_g are defined in Eqs. (12)-(16) in section 2 of the main text.

Introducing the vertical and horizontal length scales, $\mathscr{H}$ and $\mathscr{L}$, and time scale $\mathscr{T}$ as defined in Eqs. (17)-(19) of the main text we find the evolution equations for the adimensional quantities $\hat{h} = h/\mathscr{H}$, $\hat{\Psi} = \Psi/\mathscr{H}$, $\hat{\xi} = \xi/\mathscr{H}$

$$\partial_{\hat{t}} \hat{h} = -\hat{\nabla} . \hat{\mathbf{j}}_{\text{conv}} + \hat{j}_o \tag{7}$$

$$\partial_{\hat{t}} \hat{\Psi} = -\hat{\nabla} . (\phi \hat{\mathbf{j}}_{\text{conv}} + \hat{\mathbf{j}}_{\text{diff}}) + \hat{j}_g \tag{8}$$

$$\partial_{\hat{t}} \hat{\xi} = \hat{j}_s \,, \tag{9}$$

where $\hat{}$ indicates adimensional quantities, e.g. $\hat{\nabla} = \mathscr{L} \nabla$. The dimensionless convective flux $\hat{\mathbf{j}}_{\text{conv}}$ takes the form

$$\hat{\mathbf{j}}_{\text{conv}} = -\frac{\hat{h}^3}{\hat{\eta}} \hat{\nabla} \left[\frac{1}{\hat{h}^3} - \frac{1}{\hat{h}^6} - \hat{\Delta}(\hat{h} + \hat{\xi}) \right] . \tag{10}$$

with $\hat{\eta} = 1 - \phi + \mu \phi$. The dimensionless diffusive flux $\hat{\mathbf{j}}_{\text{diff}}$ takes the form

$$\hat{\mathbf{j}}_{\text{diff}} = \frac{\hat{D} \hat{h} \phi}{\hat{\eta}} \hat{\nabla} \ln \left(\frac{\phi}{1 - \phi} \right) . \tag{11}$$

The nonconserved fluxes are given in their dimensionless form by

$$\hat{j}_o = \hat{Q}_o \left[\hat{\Delta}(\hat{h} + \hat{\xi}) - \left(\frac{1}{\hat{h}^3} - \frac{1}{\hat{h}^6} \right) - \frac{1}{W_m} \ln \left(\frac{1 - \phi}{1 - \phi_{eq}} \right) \right] \tag{12}$$

$$\hat{j}_g = \hat{g} \hat{h} \phi (1 - \phi) \left(1 - \frac{\hat{h} \phi}{\hat{h}^* \phi_{eq}} \right) \left(1 - \frac{\hat{h}_u \phi_{eq}}{\hat{h} \phi} \right) \left[1 - e^{(\phi_{eq} - \hat{h} \phi)} \right] \tag{13}$$

$$\hat{j}_s = \frac{\sqrt{s}}{\tau} \left[\hat{\Delta}(\hat{h} + \hat{\xi}) + \sigma \hat{\Delta} \hat{\xi} - \frac{1}{s} \hat{\xi} \right] . \tag{14}$$

Note, that we have assumed that the friction constant of the substrate ζ is related to the bulk viscosity of the substrate η_s as $\frac{1}{\zeta} = \sqrt{\frac{\gamma_h}{\kappa_v}} \frac{1}{\eta_s}$ 2. The dimensionless parameters are

$$\hat{D} = \frac{k_B T h_a}{2\pi A a} \tag{15}$$

$$W_m = \frac{A a^3}{k_B T h_a^3} \tag{16}$$

$$\hat{Q}_o = \frac{\mathscr{T} \gamma_h Q_o}{\mathscr{L}^2} = \frac{3 Q_o \gamma_h \eta_0 h_a}{A} \tag{17}$$

$$\hat{g} = \mathscr{T} g \tag{18}$$

$$\tau = \frac{\eta_s \mathscr{L}}{\gamma_h \mathscr{T}} = \frac{\eta_s}{3\eta_0} \left(\frac{A}{\gamma_h h_a^2} \right)^{3/2} \tag{19}$$

$$\sigma = \frac{\gamma_\xi}{\gamma_h} \,. \tag{20}$$

The softness s is defined Eq. (20) of the main text. Table S1 summarizes all adimensional parameters.

S2 Initial conditions

Calculations of the biofilm evolution were started from identical initial conditions $h_0(x)$ where a small biofilm droplet of maximum

a Institut für Theoretische Physik, Universität Münster, Wilhelm-Klemm-Str. 9, 48149 Münster, Germany.
b Université Grenoble Alpes, CNRS, LIPhy, 38000 Grenoble, France.
c Center for Nonlinear Science (CeNoS), Universität Münster, Corrensstr. 2, 48149 Münster, Germany.
∗ E-mail: karin.john@univ-grenoble-alpes.fr
‡ Corresponding author. E-mail: u.thiele@uni-muenster.de

Table S1 Summary of all adimensional model parameters

Parameter	Symbol	Value
growth rate constant (as stated in the main text or the figure legends)	$\hat{g}$	
substrate softness (as stated in the main text or the figure legends)	s	
wetting parameter	W_m	5
viscosity contrast biomass-solvent	μ	10^4
diffusion constant	$\hat{D}$	$\frac{1}{2\pi}$
osmotic mobility	$\hat{Q}_o$	0.01
equilibrium biomass concentration (if not stated otherwise)	ϕ_{eq}	0.5
substrate relaxation time	τ	7.6
surface tension ratio	σ	0.1
maximal biofilm height	h^*	120
critical biofilm height for biomass production	h_u	2

height $h_{0,\max} = 20$ was approximated by a parabola of the form

$$h_0(x) = h_{0,\max} - \frac{\theta_{eq}^2}{4h_{0,\max}} x^2, \tag{21}$$

where θ_{eq} denotes the equilibrium contact angle $\theta_{eq} = \sqrt{3/5}$ of the adimensional system[1,3]. The biomass concentration is initiated as $\phi_0(x) = \phi_{eq}$, i.e. the biomass layer thickness follows the initial biofilm profile $\Psi_0(x) = \phi_{eq} h_0(x)$. The initial state of the substrate is the reference configuration, i.e. $\xi = 0$.

S3 Volume dependency of a passive biofilm with a fixed biomass

If a biofilm droplet (parabolic profile with the equilibrium contact angle $\theta_h = \sqrt{3/5}$ and with biomass concentration $\phi = \phi_{eq}$) is placed on an undeformed substrate ($\xi = 0$) and the biofilm may evolve in the absence of active biomass production ($g = 0$), the droplet will eventually adopt an equilibrium shape. During the equilibration phase the biofilm will exchange solvent with the substrate, thereby changing its volume. However, the influence of the substrate softness s on the equilibrium biofilm volume is negligible (Fig. S1).

S4 Derivation of scaling laws for the wetting ridge height $\Delta\xi_{\max}$ for passive biofilm droplets

We consider the equilibrium shape of a two-dimensional droplet (i.e. a liquid ridge) centred at $x = 0$ with fixed volume A on an elastic (rigid to very soft) substrate in the macroscopic limit. We derive here the scaling laws observed for the wetting ridge height defined as the difference in the substrate deformation at the contact line $x = r$ and position sufficiently far away from the droplet at $x = L$. The notation is identical to the main text.

S4.1 Nearly rigid elastic substrates

On a rigid substrate the elastocapillary length is smaller than the mesoscopic interface width $\mathscr{L}$, i.e. $\mathscr{L}_{ec} = \sqrt{\frac{\gamma_h}{\kappa_v}} \ll \mathscr{L}$. In that case, the size of elastic deformations of the substrate is smaller than all other length scales and decays on a scale smaller than $\mathscr{L}$. The macroscopic Young-Dupré equilibrium contact angle θ_h of the droplet is not affected by the substrate deformation and the ver-

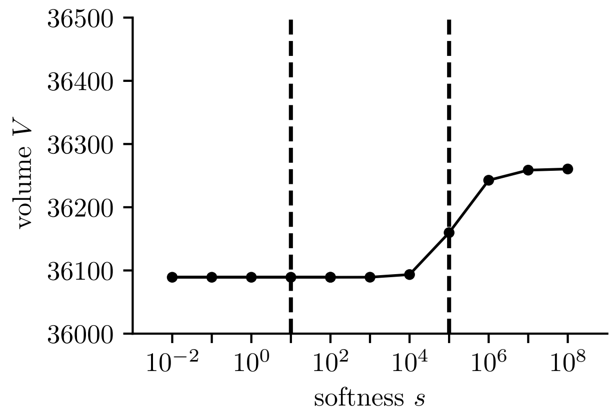

Fig. S1 Equilibrium states of passive biofilms with a fixed biomass $\int \Psi\, dx$ on soft substrates. Dependence of the biofilm volume V on substrate softness s. The vertical dashed lines separate the three scaling regimes introduced in Fig. 2 of the main text. The biomass in the droplet is $\int \Psi\, dx = \phi_{eq} V_0$ with the initial volume $V_0 = \approx 3.6 \cdot 10^4$ and $\phi_{eq} = 0.5$. The remaining parameters are given in Table S1.

tical force balance at the contact line can be expressed as

$$\kappa_v \xi_r \mathscr{L} = \gamma_h \sin\theta_h \tag{22}$$

which results in the scaling

$$\xi_r = \Delta\xi_{\max} \sim \frac{1}{\kappa_v} \sim s, \tag{23}$$

where the substrate rigidity κ_v is related to the adimensional substrates softness via $\kappa_v = \frac{\gamma_h}{\mathscr{L}^2 s}$ [cf. Eq. (20) of the main text].

S4.2 Moderately and very soft elastic substrates

On moderately and very soft substrates the elastocapillary length is larger than the mesoscopic length $\mathscr{L}$ and the equilibrium drop shape and substrate deformation can be described within a macroscopic description. For simplicity we restrict ourselves to the limit of small interface slopes $\partial_x \xi \ll 1$ and $\partial_x(h+\xi) \ll 1$. We start out by defining the potential energy $\mathscr{F}$ of the soft solid, partially covered by a liquid in the domain $0 \le x \le r$ (for similar approaches see e.g. Thiele *et al.* [3])

$$\begin{aligned} \mathscr{F} &= \int_0^r \left\{ \frac{\kappa_v}{2}\xi^2 + \gamma_s \left[1 + \frac{1}{2}(\partial_x \xi)^2\right] \right. \\ &+ \left. \gamma_h \left[1 + \frac{1}{2}(\partial_x(\xi+h))^2\right] - ph \right\} dx \\ &+ \int_r^\infty \left\{ \frac{\kappa_v}{2}\xi^2 + \gamma_{sv}\left[1 + \frac{1}{2}(\partial_x \xi)^2\right] \right\} dx + \lambda h(r). \end{aligned} \tag{24}$$

Here, γ_{sv} denotes the surface tension of the bare substrate which is related to the wetting energy by $f_{\mathrm{w}}(h_a) = \gamma_{sv} - \gamma_h - \gamma_s$ [Eq. (5) of the main text]. Further, p and λ denote Lagrangian multipliers for volume conservation and the condition that $h(x = r) = 0$, respectively. We require continuity for ξ at $x = r$ (but not continuous differentiability), i.e. x represents a corner point for ξ due to the presence of a vertical forces exerted by the contact line. The equilibrium state is determined by the vanishing variation of $\mathscr{F}$ w.r.t. h, ξ and the drop radius r.

Variation w.r.t. h results in

$$\begin{aligned} 0 &= \int_0^r \{-\gamma_h \partial_{xx}(\xi+h) - p\}\,\delta h\,dx \\ &+ \left[\gamma_h \partial_x(\xi+h)\delta h\right]_0^{r_-} + \lambda\,\delta h(r_-) \\ &= \int_0^r \{-\gamma_h \partial_{xx}(\xi+h) - p\}\,\delta h\,dx \\ &+ \left[\gamma_h \partial_x(\xi+h) + \lambda\right]_{r_-}\delta h\,, \end{aligned} \tag{25}$$

where we have used the parity symmetry of the droplet, i.e. $\partial_x(\xi+h)=0$ at $x=0$. From Eq. (25) we find the Lagrange multiplier

$$\lambda = -\gamma_h \partial_x(\xi+h) \quad \text{at} \quad x=r_-, \tag{26}$$

and in the bulk for $0 \le x < r$ the Laplace law

$$p = -\gamma_h \partial_{xx}(\xi+h)\,. \tag{27}$$

Variation w.r.t. r results in the equivalent of the horizontal force balance

$$\begin{aligned} 0 &= \left\{\frac{\kappa_v}{2}\xi^2 + \gamma_s\left[1+\frac{1}{2}(\partial_x\xi)^2\right] + \gamma_h\left[1+\frac{1}{2}(\partial_x(\xi+h))^2\right]\right. \\ &- \left. ph\right\}_{r_-}\delta r \\ &- \left\{\frac{\kappa_v}{2}\xi^2 + \gamma_{sv}\left[1+\frac{1}{2}(\partial_x\xi)^2\right]\right\}_{r_+}\delta r + \lambda\,\partial_x h(r_-)\delta r\,. \end{aligned} \tag{28}$$

The notation r_+ and r_- indicates that evaluation of derivatives takes place on the right and the left side at $x=r$, respectively. Simplifying Eq. (28) leads to

$$\begin{aligned} 0 &= \left\{\gamma_s\left[1+\frac{1}{2}(\partial_x\xi)^2\right] + \gamma_h\left[1+\frac{1}{2}(\partial_x(\xi+h))^2\right]\right\}_{r_-} - \\ &\left\{\gamma_{sv}\left[1+\frac{1}{2}(\partial_x\xi)^2\right]\right\}_{r_+} + \lambda\,\partial_x h(r_-)\,. \end{aligned} \tag{29}$$

with λ given by Eq. (26).

Variation w.r.t. ξ results in

$$\begin{aligned} 0 &= \int_0^r \{-\gamma_s\partial_{xx}\xi - \gamma_h\partial_{xx}(\xi+h) + \kappa_v\xi\}\,\delta\xi\,dx + \\ &\int_r^\infty \{-\gamma_{sv}\partial_{xx}\xi + \kappa_v\xi\}\,\delta\xi\,dx + \\ &\left[(\gamma_s\partial_x\xi + \gamma_h\partial_x(\xi+h))\delta\xi\right]_0^{r_-} + \left[\gamma_{sv}\partial_x\xi\,\delta\xi\right]_{r_+}^\infty\,. \end{aligned} \tag{30}$$

The contributions at $x=0$ vanish by symmetry, i.e. $\partial_x\xi=0$ and $\partial_x(\xi+h)=0$ at $x=0$. Furthermore, $\partial_x\xi=0$ as $x\to\infty$. At $x=r$ we recover the vertical force balance

$$0 = \gamma_s\partial_x\xi|_{r_-} + \gamma_h\partial_x(\xi+h)|_{r_-} - \gamma_{sv}\partial_x\xi|_{r_+}\,. \tag{31}$$

In the bulk the equations

$$0 = -\gamma_s\partial_{xx}\xi - \gamma_h\partial_{xx}(\xi+h) + \kappa_v\xi \quad \text{for} \quad 0\le x<r \tag{32}$$

$$0 = -\gamma_{sv}\partial_{xx}\xi + \kappa_v\xi \quad \text{for} \quad r<x \tag{33}$$

hold.

Using the Laplace equation (27) and Eqs. (32) and (33) we find the solutions for the substrate deformation and the droplet profile for $0\le x<r$ after two integration steps (using $\partial_x(\xi+h)=0$ at $x=0$ and $h=0$ and $\xi=\xi_r$ at $x=r$). They are

$$\xi(x) = \left(\xi_r + \frac{p}{\kappa_v}\right)\frac{\cosh(x/\mathscr{L}_{ec,1})}{\cosh(r/\mathscr{L}_{ec,1})} - \frac{p}{\kappa_v}, \tag{34}$$

$$h(x) = \frac{1}{2}\frac{P}{\gamma_h}(R^2-x^2) + \xi_r - \xi(x), \tag{35}$$

and for the substrate deformation profile for $r<x$

$$\xi(x) = \xi_r e^{-(x-r)/\mathscr{L}_{ec,2}}\,. \tag{36}$$

$\mathscr{L}_{ec,1} = \sqrt{\gamma_s/\kappa_v}$ and $\mathscr{L}_{ec,2} = \sqrt{\gamma_{sv}/\kappa_v}$ denote elastocapillary lengths. Introducing the expressions (34)-(36) into the vertical force equilibrium (31) we find

$$0 = -pr + \sqrt{\gamma_{sv}\kappa_v}\xi_r + \sqrt{\gamma_s\kappa_v}\left(\frac{p}{\kappa_v} + \xi_r\right)\tanh(r/\mathscr{L}_{ec,1})\,. \tag{37}$$

Moderately soft substrates: For moderately soft substrates ($r \gg \mathscr{L}_{ec}$) the vertical force balance reduces to

$$0 = -pr + \sqrt{\kappa_v}\xi_r\left(\sqrt{\gamma_s} + \sqrt{\gamma_{sv}}\right), \tag{38}$$

where we have used $\tanh(r/\mathscr{L}_{ec,1}) \approx 1$ and $p(\sqrt{\gamma_s/\kappa_v} - r) = (\mathscr{L}_{ec,1} - r) \approx -pr$. Assuming that the droplet shape and Laplace pressure do not significantly change from the rigid regime we find the height of the wetting ridge ξ_r (which for $L \gg \mathscr{L}_{ec,2}$ is identical to the height difference $\Delta\xi_{\max}$) to be given by

$$\xi_r = \Delta\xi_{\max} = \frac{pr}{\sqrt{\kappa_v}\left(\sqrt{\gamma_s} + \sqrt{\gamma_{sv}}\right)} \sim \kappa_v^{-1/2} \sim s^{1/2}\,. \tag{39}$$

Very soft substrates: In the limit of very soft substrates ($r \ll \mathscr{L}_{ec}$) the vertical force balance reduces to lowest order to

$$\xi_r = \frac{pr^3}{3\gamma_s\sqrt{\gamma_{sv}}}\sqrt{\kappa_v}, \tag{40}$$

i.e. the absolute height of the wetting ridge scales as $\xi_r \sim \kappa_v^{1/2} \sim s^{-1/2}$. To obtain Eq. (40) we have first used the expansion up to third order in $r/\mathscr{L}_{ec,1}$

$$\tanh\left(\frac{r}{\mathscr{L}_{ec,1}}\right) \approx \frac{r}{\mathscr{L}_{ec,1}} - \frac{1}{3}\left(\frac{r}{\mathscr{L}_{ec,1}}\right)^3 \tag{41}$$

and then the approximation

$$\sqrt{\gamma_{sv}} + \sqrt{\gamma_s}\left[\frac{r}{\mathscr{L}_{ec,1}} - \frac{1}{3}\left(\frac{r}{\mathscr{L}_{ec,1}}\right)^3\right] \approx \sqrt{\gamma_{sv}}\,. \tag{42}$$

Recall that the wetting ridge height difference is given by

$$\Delta\xi_{\max} = \xi(x=r) - \xi(x=L), \tag{43}$$

where L denotes a position sufficiently far away from the droplet ($r \ll L \ll \mathscr{L}_{ec,2}$). In this limit the substrate deformation outside of the droplet (36) at $x = L$ has not yet decayed to zero as the elastocapillary length $\mathscr{L}_{ec,2}$ is large. Using Eq. (43) with Eq. (36) results in

$$\begin{aligned}\Delta\xi_{\max} &= \xi_r\left(1 - e^{-(L-r)/\mathscr{L}_{ec,2}}\right) \\ &\approx \xi_r \frac{L-r}{\mathscr{L}_{ec,2}} = \xi_r(L-r)\sqrt{\frac{\kappa_v}{\gamma_{sv}}} \\ &\approx \xi_r L\sqrt{\frac{\kappa_v}{\gamma_{sv}}}. \end{aligned} \tag{44}$$

Combining Eqs. (40) and (44) gives

$$\Delta\xi_{\max} = \frac{pr^3L}{3\gamma_s\gamma_{sv}}\kappa_v \tag{45}$$

which results in the scaling of wetting ridge height difference

$$\Delta\xi_{\max} \sim \kappa_v \sim s^{-1} \tag{46}$$

assuming constant pressure and droplet radius not significantly different from the liquid regime.

Influence of boundary conditions: In numerical simulations, the computational domain is finite with Neumann boundary conditions (BCs; $\partial_x\xi = 0$ at $x = L$). In the very soft case $r/\mathscr{L}_{ec,2}$ the BCs may influence the scaling behavior. Using Neumann BCs the substrate deformation outside of the droplet is given by

$$\xi(x) = \xi_r \frac{\cosh\left[(x-L)/\mathscr{L}_{ec,2}\right]}{\cosh\left[(r-L)/\mathscr{L}_{ec,2}\right]} \quad \text{for} \quad r < x < L \tag{47}$$

Then the vertical force balance (31) becomes

$$\begin{aligned} 0 &= -pr + \frac{\gamma_s}{\mathscr{L}_{ec,1}}\left(\frac{p}{\kappa_v} + \xi_r\right)\tanh\left(r/\mathscr{L}_{ec,1}\right) \\ &- \frac{\gamma_{sv}}{\mathscr{L}_{ec,2}}\xi_r \tanh\left[(r-L)/\mathscr{L}_{ec,2}\right]. \end{aligned} \tag{48}$$

Again, expanding tanh up to 3rd order we find to lowest order for ξ_r

$$\xi_r = \frac{r^3 p}{3\gamma_s L}, \tag{49}$$

i.e. the absolute wetting ridge height is independent of the substrate rigidity κ_v. For the wetting ridge height difference we find

$$\begin{aligned}\Delta\xi_{\max} &= \xi_r\left(1 - \frac{1}{\cosh\left[(L-r)/\mathscr{L}_{ec,2}\right]}\right) \approx \xi_r\frac{(L-r)^2}{2\mathscr{L}_{ec,2}^2} \\ &\approx \xi_r\frac{L^2}{2\mathscr{L}_{ec,2}^2} \\ &\approx \frac{r^3 pL}{6\gamma_s\gamma_{sv}}\kappa_v \sim \kappa_v \sim s^{-1}, \end{aligned} \tag{50}$$

where we have used Eq.(49). The scaling $\Delta\xi_{\max} \sim s^{-1}$ is therefore a general result, whereas the scaling of the absolute wetting ridge height ξ_r depends on the chosen boundary conditions.

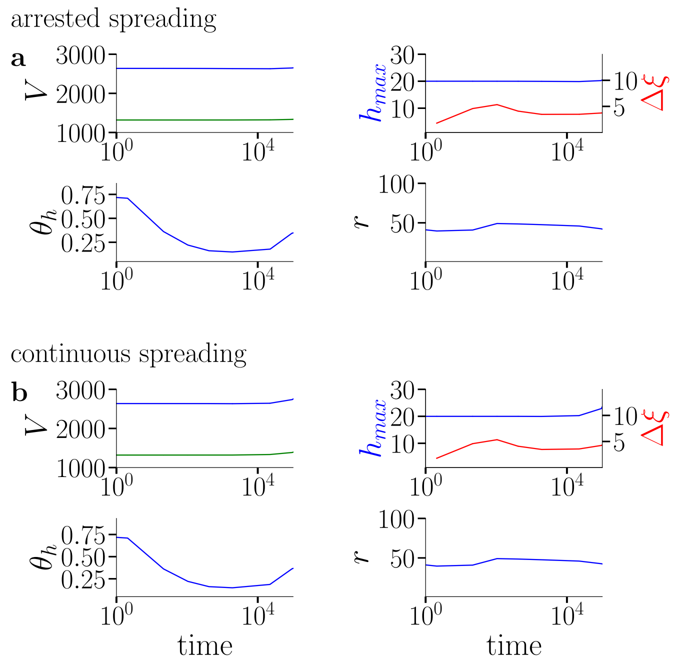

Fig. S2 Spreading of active biofilms on soft substrates on short time scales at low (a, $g = 1.3\cdot10^{-6}$) and high (b, $g = 5.3\cdot10^{-6}$) biomass growth rate constant. Shown is the evolution at short times of biofilm and biomass volume (V, blue and green, respectively), maximal biofilm (h_{max}, blue) and wetting ridge ($\Delta\xi$, red) heights, macroscopic contact angle θ_h and biofilm extension (r). The substrate softness is $s = 10^4$ and remaining parameters are as given in Table S1.

S5 Measurement of the spreading velocity and the contact angle

In order to measure the lateral spreading velocity of the biofilm we determined first the radius r of the biofilm as the position of the inflection point in the biofilm front. The velocity was then determined from the slope of the curve $r(t)$.

To calculate the contact angle θ_h of the biofilm edge with the substrate, we fitted the droplet profile (in the arrested and spreading case) in the relevant front region with a parabola of the form $f(x) = -a(x-b)^2 + c$. The assumed form of the fit function is a parabola given by

$$f(x) = -a(x-b)^2 + c.$$

The contact angle was then determined as the slope of the parabola where the biofilm front meets the substrate, i.e. $\theta_h = 2\sqrt{ac}$.

S6 Evolution of biofilm droplets on short time scales

Fig. S2 (a,b) characterises the arrested and continuous spreading regimes at short times in terms of the evolution of the biofilm volume and total biomass (V , blue and green curves, respectively), the maximal film height h_{max} and wetting ridge height $\Delta\xi$, the contact angle of the biofilm edge θ_h, and the lateral biofilm extension r. The main characteristic at short times is a decrease in the contact angle, whereas all other observables do not change considerably. This behaviour holds for the arrested case (low growth rate constant) and the continuous spreading case (high growth rate constant).

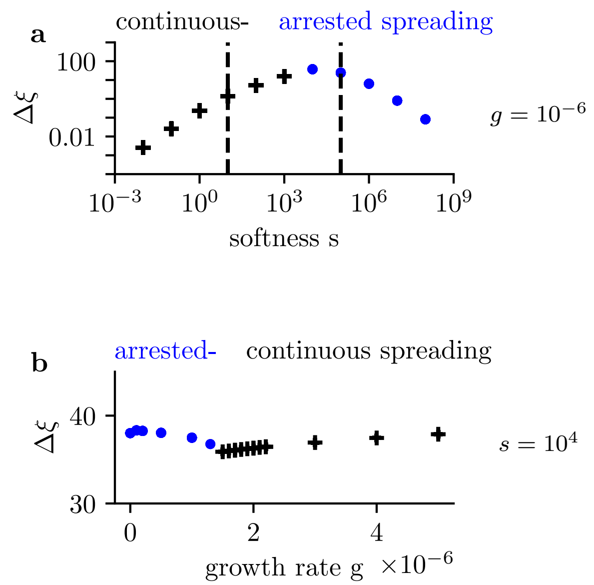

Fig. S3 Dependence of the wetting ridge height on the substrate softness s (a) and biomass growth rate constant g (b). The vertical dashed lines separate the three scaling regimes as explained in Fig. 2 of the main text. The remaining parameters are given in Table S1.

S7 Dependency of the wetting ridge height on the substrate softness s for an active biofilm

To get a better understanding of the influence of the substrate softness on the spreading behaviour of biofilms with biomass production ($g > 0$) we measure the wetting ridge height for spreading and stationary biofilms (Fig. S3 (a)). The wetting ridge height is mainly determined by the substrate softness, and, even in the active case, a similar scaling behaviour as in the passive droplet case can be observed (cf. Fig. 2 (d) of the main text). Interestingly the transition between spreading and arrested regime coincides with the transition from the soft to the very soft (liquid-like) substrate, where the biofilm starts to sink into the substrate, and the height of the wetting ridge starts to decrease. The growth rate has only a minor influence on the wetting ridge height [Fig. S3 (b)]. However, here the transition of the arrested to the spreading regime (by increasing the growth rate constant g) is marked by a minimum in the height of the wetting ridge.

References

1 C. Henkel, J. H. Snoeijer and U. Thiele, *Soft Matter*, 2021, **17**, 10359–10375.

2 C. Henkel, M. H. Essink, T. Hoang, G. J. van Zwieten, E. H. van Brummelen, U. Thiele and J. H. Snoeijer, *Proceedings of the Royal Society A: Mathematical, Physical and Engineering Sciences*, 2022, **478**, 20220132.

3 U. Thiele, J. H. Snoeijer, S. Trinschek and K. John, *Langmuir*, 2018, **34**, 7210–7221.